Available online at www.sciencedirect.com
ScienceDirect
Journal of Sound and Vibration 316 (2008) 164–179
JOURNAL OF SOUND AND VIBRATION
www.elsevier.com/locate/jsvi

# Dynamic instability of a thin circular plate with friction interface and its application to disc brake squeal

Jaeyoung Kang*, Charles M. Krousgrill, Farshid Sadeghi

*School of Mechanical Engineering, Purdue University, 585 Purdue Mall, West Lafayette, IN 47907-2088, USA*

Received 23 July 2006; received in revised form 25 December 2007; accepted 18 February 2008
Handling Editor: S. Bolton
Available online 3 April 2008

**Abstract**

The mathematical formulation for determining the dynamic instability due to transverse doublet modes in the self-excited vibration of a thin annular plate is presented in this paper. An analytical approach is developed to obtain the stability results from the eigenvalue problem of a stationary disc with a finite contact area. The approach uses the eigenfunctions of transverse doublet modes in classical plate theory and establishes the formulation of modal instability due to the modal-interaction of a doublet mode pair. The one-doublet mode model of a disc and a discrete model equivalent to the one-doublet mode model are proposed for providing a more fundamental understanding of the onset of squeal. The analytical models are validated through a comparison of results from a modal expansion model obtained from finite element component models. Throughout the analytical investigation, the pad arc length is found to be a critical design parameter in controlling squeal propensity.


## 1. Introduction

Friction is the source of squeal noise in a brake system. Friction force on contact interface produces non-conservative work that can eventually lead to unstable oscillations. An effective model for friction-induced vibration is constructed from the system equations of motion using a linearized friction and contact stiffness model. The dynamic instability near a steady sliding equilibrium position can be determined from the appearance of the positive real parts of eigenvalues of the linearized model as extensively reviewed in the review article [1].

In mathematical interpretation, the non-conservative frictional work produces a non-symmetric stiffness matrix in the linearized equations of motion that is necessary for the appearance of eigenvalues with positive real parts. The non-symmetric elements in the stiffness matrix of brake system model can arise from the non-conservative nature of follower forces and friction-couples. Mottershead and Chan [2] used frictional follower loads to study the flutter instability of doublet modes of a finite element non-rotating disc model. Also, Mottershead [3] extensively introduced several follower force friction models in his review article. However,

*Corresponding author.
*E-mail address:* kang28@purdue.edu (J. Kang).

0022-460X/$ - see front matter © 2008 Elsevier Ltd. All rights reserved.
doi:10.1016/j.jsv.2008.02.041

the influence of follower forces on squeal propensity has been seen to be marginal. Flint and Hulten [4] developed a stationary disc brake model with follower force and friction-couple components and concluded that the relative effect of follower forces was negligible. Heilig and Wauer [5] developed a simplified rotating disc brake model with two different contact models, global contact and local gradient contact models, where the local gradient contact model describes the direction change of the contact forces corresponding to the disc deformation. Therefore, the contact forces of the local gradient contact model are follower forces. From their numerical results, they also concluded "the differences in the results between the global and local gradient contact modeling are marginal ($<0.1\%$) and not visible in the plots". Ouyang and Mottershead [6] have shown that the follower force term is many times smaller than the friction-couple term in disc brake system.

In contrast, the friction-couple mechanism is considered to be a significant brake squeal leading factor in producing vibrations. Since the friction-couple mechanism is derived from the undeformed contact kinematics (or global contact model), the global contact model is sufficient in describing the contact mechanics of the brake system. Ouyang and his coworkers [7] provided an extensive review on the automotive disc brake squeal analysis described by the friction-couple mechanism in a linearized set of equations of motion.

One of the primary sources of nonlinearities in brake system models is the nonlinear load-deflection behavior of the friction material. A small change of preload can lead to a significant change in the linearized contact stiffness. Vanderlugt [8] in his experimental work showed that the vibration modes leading to squeal can be modified as contact stiffness changes with respect to brake pressure variation. This implies that the stability of each mode depends on contact stiffness variation. In order to investigate the modal stability behavior and its stability boundary from the linearized equations of motion, Chowdhary et al. [9] treated contact stiffness as a system parameter and solved the eigenvalue sensitivity problem of disc brake system on the dynamic instability of the steady-sliding response. Their contribution to brake squeal research has been to show the role of mode-coupling and mode-merging on the stability boundaries in the stiffness-friction plane. Later, Huang et al. [10] presented the qualitative relations between mode-coupling and mode-merging and showed that the compatibility of mode shapes needed for mode coupling is one of the factors dictating the onset of squeal in drum brake system. However, numerical results from their analysis did not establish the generalized squeal theory associated with modal interaction.

In the present study, a simplified mathematical disc model is constructed on the basis of the physical disc brake system that was studied experimentally and numerically by Vanderlugt [8]. Since the unstable modes on squeal frequencies were found to be disc doublet modes in his work, the one-doublet mode model of a thin annular plate representing a brake rotor is developed and investigated. For the practical purpose, the system parameters and the component disc natural frequencies are obtained from the measured data and the finite element (FE) analysis in Vanderlugt's work [8]. The modal results obtained from the finite element method showed the non-coincidence of the two natural frequencies in a doublet mode. The frequency separation of the component disc mode pair will be the focus of this study and the corresponding modal stability boundary will be solved with respect to contact stiffness variation.

The main objective of the work presented in this paper is to analytically describe the modal instability of disc brake system. This work provides the formulation for the squeal onset of brake geometry that has not been addressed in any previous papers. The essence of the formulation is to provide the fundamental design concept of reducing squeal occurrence in disc brake system. Also, this work provides the physical interpretation for the formulation of squeal onset. For better physical interpretation, a discrete model representing the modification of Hoffmann's model [11] is introduced, where this simplified model is shown to be mathematically equivalent to the doublet mode model.

## 2. Model development

### 2.1. Equations of motion

The dynamic instability due to circumferential friction between a stationary thin annular plate and two fixed annular sector contact interfaces under steady-sliding conditions are investigated. Rotational effects are not considered by assuming that the rotation speed is near the critical speed (in the mid range) [12] where the gyroscopic destabilizing effect and the radial dissipative effect cancel out. The effect of frictional follower force

is neglected on the basis that contact stiffness term is much larger than pre-stress term in the stiffness matrix [4–6]. Here, the annular plate is subject to clamped boundary condition at inner radius and free boundary condition at outer radius. The corresponding equation of motion for the transverse motion, $w(\vec{x}, t)$ of the annular plate can be written as

$$\rho h \frac{\partial^2 w(\vec{x}, t)}{\partial t^2} + D\nabla^4 w(\vec{x}, t) = 0, \tag{1}$$

where

$$\nabla^4 = \left(\frac{\partial^2}{\partial r^2} + \frac{\partial}{r\partial r} + \frac{\partial^2}{r^2\partial\theta^2}\right)^2, \quad D = \frac{Eh^3}{12(1-v^2)}, \tag{2}$$

and $E$, $\rho$ and $v$ are the Young modulus, the mass density and the Poisson ratio, respectively, of the disc material. The transverse displacement can be written in the following truncated modal expansion:

$$\begin{aligned} w(\vec{x}, t) &\cong \sum_{n=1}^{N/2} R_n(r)\{\cos(n\theta)q_{2n-1}(t) + \sin(n\theta)q_{2n}(t)\} \\ &\equiv \sum_{j=1}^{N} \phi_{z,j}(r, \theta)q_j(t), \end{aligned} \tag{3}$$

where $R_n(r) = A_nJ_n(\beta r) + E_nY_n(\beta r) + B_nI_n(\beta r) + F_nK_n(\beta r)$. $J_n$ and $Y_n$ are the ordinary Bessel functions of the first and second kind, and $I_n$ and $K_n$ are the modified Bessel functions of the first and second kind. $n$ is the number of nodal diameters on a vibrating annular plate and is referred to as the mode number.

To satisfy the clamped-free boundary condition, the displacement and the slope of displacement must be zero at inner radius and the moment and shear force must be zero at outer radius [13]. The algebraic equations resulting from enforcing the four boundary conditions are:

$$\begin{bmatrix} J_n(\beta a) & Y_n(\beta a) & I_n(\beta a) & K_n(\beta a) \\ (p_nJ_n - J_{n+1})(\beta a) & (p_nY_n - Y_{n+1})(\beta a) & (p_nI_n + I_{n+1})(\beta a) & (p_nK_n - K_{n+1})(\beta a) \\ \{(t_n-1)J_n + s_nJ_{n+1}\}(\beta b) & \{(t_n-1)Y_n + s_nY_{n+1}\}(\beta b) & \{(t_n+1)I_n - s_nI_{n+1}\}(\beta b) & \{(t_n+1)K_n + s_nK_{n+1}\}(\beta b) \\ \{p_n(t_n+1)J_n - (np_ns_n+1)J_{n+1}\}(\beta b) & \{p_n(t_n+1)Y_n - (np_ns_n+1)Y_{n+1}\}(\beta b) & \{p_n(t_n-1)I_n + (np_ns_n-1)I_{n+1}\}(\beta b) & \{p_n(t_n-1)K_n - (np_ns_n-1)K_{n+1}\}(\beta b) \end{bmatrix} \begin{Bmatrix} A_n \\ E_n \\ B_n \\ F_n \end{Bmatrix} = \begin{Bmatrix} 0 \\ 0 \\ 0 \\ 0 \end{Bmatrix}, \tag{4}$$

where

$$p_n(\beta r) = n/\beta r, \tag{5}$$

$$s_n(\beta r) = (1-v)/\beta r, \tag{6}$$

$$t_n(\beta r) = n(n-1)(1-v)/(\beta r)^2. \tag{7}$$

The values of $\beta$ corresponding to the zero determinant of the matrix in Eq. (4) are sought for the $n$th nodal diameter mode and are denoted as $\beta_n$. The coefficient vectors, $\{A_n, E_n, B_n, F_n\}^{\mathrm{T}}$ corresponding to $\beta_n$ are obtained and assigned to the radial component of the eigenfunction, $R_n(r)$.

For disc brake systems with double-sided pistons, brake pressure is applied symmetrically on both sides of the disc. In a single-piston floating-caliper system, the caliper slides from side-to-side as brake pressure is applied. Here, the preloads exerted on the back-plates of two pads by brake pressure are assumed to be identical under steady braking condition as shown in Fig. 1. The pre-stress is assumed to be uniformly

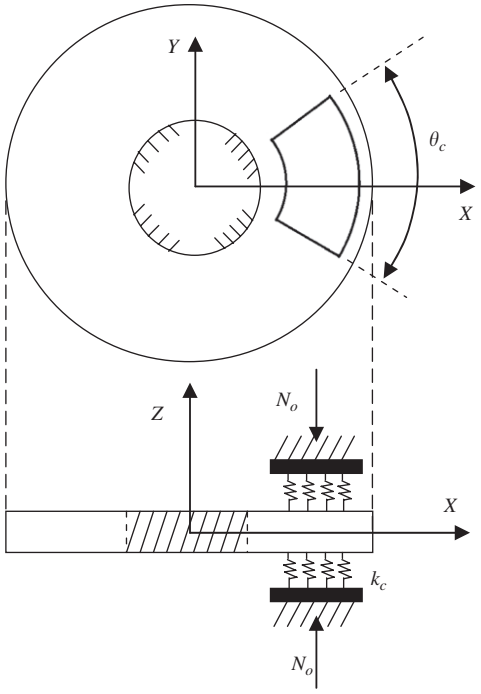


Fig. 1. Description of a stationary thin annular plate with annular sector friction interface; $N_o$ is the preload acting on the top pad and the bottom pad, symmetrically.

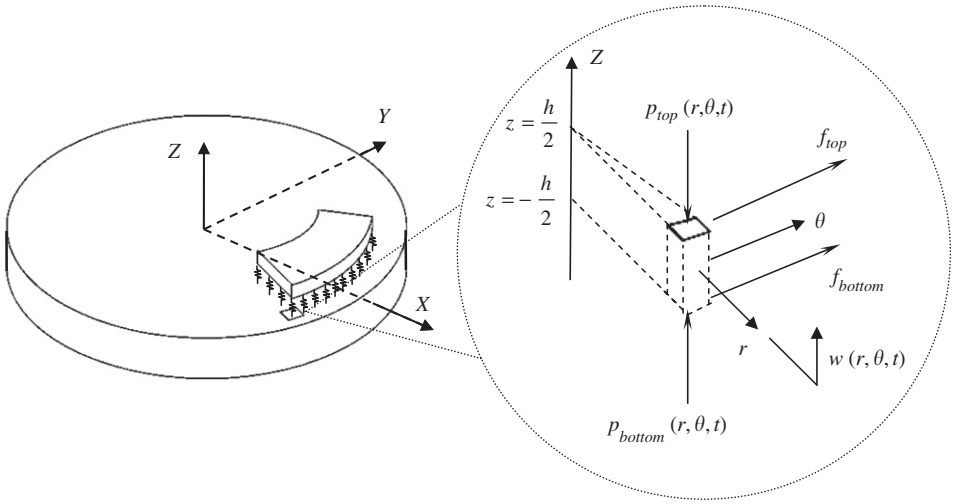


Fig. 2. Description of contact stresses on a specific location of contact area, $A_{CS}$.

distributed over the contact area such as $p_o = N_o/A_{CS}$ where $N_o$ is the preload and $A_{CS}$ is the contact area. Also, friction coefficient is assumed to be uniformly constant over the contact area of the disc. The vertical contact and friction stresses on the top and bottom contact node in Fig. 2 will be obtained from the static plus vibrating fluctuation stresses, respectively, such that

$$p_{\text{top}}(r,\theta,t) = p_o - k_c w(r,\theta,t), \tag{8}$$

$$p_{\text{bottom}}(r,\theta,t) = p_o - k_c w(r,\theta,t), \tag{9}$$

$$f_{\text{top}}(r,\theta,t) = \mu p_{\text{top}}, \tag{10}$$

$$f_{\text{bottom}}(r,\theta,t) = \mu p_{\text{bottom}}. \tag{11}$$

Therefore, the virtual work done by contact forces over the contact area is expressed in the following form:

$$\begin{aligned}\delta W_{\text{cs}} = &\int_{\text{cs}} [-(p_o + k_c w)\delta w - f_{\text{top}}\delta u_\theta] r \,\mathrm{d}r \,\mathrm{d}\theta \\ &+ \int_{\text{cs}} [(p_o - k_c w)\delta w - f_{\text{bottom}}(-\delta u_\theta)] r \,\mathrm{d}r \,\mathrm{d}\theta,\end{aligned} \tag{12}$$

where $\int_{\text{cs}} \equiv \int_{-\theta_c/2}^{\theta_c/2} \int_{r_i}^{r_o}$ and $u_\theta = -h/2(\partial w/r\partial\theta)$.

The equations of motion of the disc brake system are derived from the assumed modes approach using the displacement modal expansion of Eq. (3) and

$$\frac{\mathrm{d}}{\mathrm{d}t}\left[\frac{\partial T}{\partial \dot{q}_i}\right] + \frac{\partial U}{\partial q_i} = \sum_{j=1}^{N} Q_{ij}(q_j), \tag{13}$$

where

$$T = \frac{\rho h}{2}\int_0^{2\pi}\int_a^b \left[\frac{\partial w(r,\theta,t)}{\partial t}\right]^2 r \,\mathrm{d}r \,\mathrm{d}\theta, \tag{14}$$

$$\delta W_{\text{cs}} \equiv \sum_{i=1}^{N}\sum_{j=1}^{N} Q_{ij}(q_j)\delta q_i. \tag{15}$$

Here the virtual work due to friction over the contact shown in Fig. 2 produces the generalized forces $Q_{ij}$ in Eq. (13). The kinetic energy, $T$ is decomposed into each coordinate by substituting Eq. (3) into $T$ with mass normalization, $\rho h\pi \int_a^b R_i^2 r \,\mathrm{d}r \equiv 1$. Consequently, $\partial U/\partial q_i$ becomes the square of a circular natural frequency of the stationary disc, $\omega_i^2$, which is obtained from Eq. (4). Therefore, the linearized equation of Eq. (13) is obtained in the following $(N \times N)$ matrix form:

$$\{\ddot{q}\} + ([\omega^2] + [A])\{q\} + [B]\{q\} = 0, \tag{16}$$

where $[\omega^2] = \text{diag}(\omega_n^2)$ is the natural frequency matrix of the component disc, $[A] = [A]^{\text{T}}$ is the contact stiffness matrix. $[B] \neq [B]^{\text{T}}$ is the non-symmetric non-conservative work matrix produced by friction-moment.

### 2.2. Reduced-order model: one-doublet modes approximation

The focus of this work will be on using a single doublet mode pair model for the prediction of squeal. Here, the $n$th doublet mode pair to be used is

$$\phi_{z,1} = R_n(r)\cos(n\theta), \tag{17}$$

$$\phi_{z,2} = R_n(r)\sin(n\theta). \tag{18}$$

From Eq. (16), the linearized equations of motion for the one-doublet mode takes on the following matrix form:

$$\underline{\ddot{q}} + [\omega^2]\,\underline{q} + [A]\,\underline{q} + [B]\,\underline{q} = 0, \tag{19}$$

where

$$\underline{q} = \{q_{2n-1}, q_{2n}\}^{\text{T}}, \tag{20}$$

$$[\omega^2] = \begin{bmatrix} \omega_{2n-1}^2 & 0 \\ 0 & \omega_{2n}^2 \end{bmatrix}, \tag{21}$$

$$[A] = k_c \tilde{R}_n^z \int_{-\theta_c/2}^{\theta_c/2} \begin{bmatrix} \cos^2 n\theta & 0 \\ 0 & \sin^2 n\theta \end{bmatrix} \mathrm{d}\theta, \tag{22}$$

$$[B] = \mu k_c n \tilde{R}_n^\theta \int_{-\theta_c/2}^{\theta_c/2} \begin{bmatrix} 0 & -\sin^2 n\theta \\ \cos^2 n\theta & 0 \end{bmatrix} \mathrm{d}\theta, \tag{23}$$

$$\tilde{R}_n^z = 2 \int_{r_i}^{r_o} \{R_n^2(r) r\} \, \mathrm{d}r, \tag{24}$$

$$\tilde{R}_n^\theta = -2 \int_{r_i}^{r_o} \left\{ \frac{h}{2} R_n^2(r) \right\} \mathrm{d}r. \tag{25}$$

Using $\{q(t)\} = \{V\} \mathrm{e}^{\lambda t}$, the characteristic equation for the system becomes

$$\det([H + \lambda^2(I)]) = 0, \tag{26}$$

where $[H] \equiv [\omega^2] + [A] + [B]$ and $\lambda$ is eigenvalues determining the dynamic instability of the brake system. The appearance of positive real parts of $\lambda$ indicates an unstable steady sliding equilibrium. Solving for the eigenvalues from Eq. (26) shows that positive real parts and non-zero imaginary parts occur when

$$\mu > \mu_{\mathrm{cr}} = \frac{\left|\Omega_{2n-1}^2 - \Omega_{2n}^2\right|}{k_c \left|\tilde{R}_n^\theta\right| \sqrt{(n\theta_c)^2 - \sin^2(n\theta_c)}}, \tag{27}$$

where $\Omega_{2n-1}$ and $\Omega_{2n}$ are the stiffness-coupled circular natural frequencies obtained from Eqs. (21) and (22) such that

$$\Omega_{2n-1}^2 = \omega_{2n-1}^2 + k_c \tilde{R}_n^z \int_{-\theta_c/2}^{\theta_c/2} (\cos^2 n\theta) \, \mathrm{d}\theta, \tag{28}$$

$$\Omega_{2n}^2 = \omega_{2n}^2 + k_c \tilde{R}_n^z \int_{-\theta_c/2}^{\theta_c/2} (\sin^2 n\theta) \, \mathrm{d}\theta. \tag{29}$$

The works of [9,10] provide some insight on the relationship of the critical friction coefficient to the frequency separation $(\Omega_{2n-1}^2 - \Omega_{2n}^2)$. In these works, the modal stability boundary associated with two veering modes from overall system stability boundary was identified and it was concluded that mode-veering of two adjacent modes was directly related to squeal propensity. Here, their qualitative observations can be explained by the analytical formulation of Eq. (27) such that the closeness of frequencies of a doublet mode pair is expected to increase squeal propensity.

The frequency separation on mode-veering is the difference between the two stiffness-coupled natural frequencies ($\mu = 0$) such that

$$\Omega_{2n-1}^2 - \Omega_{2n}^2 = (\omega_{2n-1}^2 - \omega_{2n}^2) + \frac{k_c \tilde{R}_n^z}{n} \sin(n\theta_c), \tag{30}$$

From a design perspective, the contact span angle $\theta_c$ is the only controllable system parameter in Eq. (30). Therefore, the specific values of $\theta_c$ minimizing $\Omega_{2n-1}^2 - \Omega_{2n}^2$ (or, equivalently minimizing $\mu_{\mathrm{cr}}$) is crucial in the design of disc brake system. Those contact span angles will be referred to as the critical contact span angle $\theta_c^{\mathrm{cr}}$. The critical contact span angle can be found from Eq. (30) such that

$$\sin(n\theta_c^{\mathrm{cr}}) = \frac{n}{\tilde{R}_n^z} \frac{(\omega_{2n}^2 - \omega_{2n-1}^2)}{k_c}. \tag{31}$$

For a perfectly axi-symmetric circular plate, we have $\omega_{2n-1}^2 = \omega_{2n}^2$, and therefore, contact span angles leading to $\sin(n\theta_c^{\mathrm{cr}}) = 0$ produce $\mu_{\mathrm{cr}} = 0$. Therefore, $\sin(n\theta_c) = 0$ is the condition for the critical contact span angles of a perfectly axi-symmetric disc. For a physical disc, however, non-zero component frequency

separation ($\omega_{2n-1} \neq \omega_{2n}$) in a doublet mode pair is likely to exist. In general, $(\omega_{2n}^2 - \omega_{2n-1}^2)/k_c$ is small due to nearly axi-symmetry and relatively large value of contact stiffness $k_c$. Critical contact span angles for a nearly axi-symmetric disc are found from Eq. (31); however $\sin(n\theta_c) = 0$ can be used as a reasonable approximation.

### 2.3. Disc doublet discrete model

For a better understanding of mode-veering and modal instability, a simplified discrete model is introduced here. A two-degree-of-freedom spring-mass model shown in Fig. 3a has been proposed [11] to demonstrate the mode-coupling type instability. The spring-mass model includes two system springs ($k_1$, $k_2$) and one contact spring ($k_o$) between a single mass and a single traveling surface. The oscillation of the system produces normal force variation and friction force variation on single point contact and it can lead to self-excited vibration. For the purpose of the mathematical equivalency to the one-doublet mode model as described in the following discussion, this model will be modified.

The off-diagonal elements in the contact stiffness matrix [$A$] of Eq. (22) for the one-doublet mode model are seen to be zero. This implies that two modes do not have contact stiffness-coupling. To make the discrete model mathematically equivalent to the one-doublet mode model, two contact springs should exist in orthogonal directions since the orthogonal arrangement of two contact springs produces the diagonal contact stiffness-coupling matrix in the discrete model. The discrete model shown in Fig. 3b is the result of this contact spring re-arrangement. The equations of motion of the system in Fig. 3b can be shown to be of the form:

$$\ddot{\underline{q}} + [\hat{\omega}^2]\underline{q} + [\hat{A}]\underline{q} + \eta[\hat{B}_\theta]\underline{q} = 0, \tag{32}$$

where

$$[\hat{\omega}^2] = \begin{bmatrix} k_1 & 0 \\ 0 & k_2 \end{bmatrix}, \tag{33}$$

$$[\hat{A}] = \begin{bmatrix} k_x & 0 \\ 0 & k_y \end{bmatrix}, \tag{34}$$

$$[\hat{B}_\theta] = \begin{bmatrix} 0 & -k_y \\ k_x & 0 \end{bmatrix} \tag{35}$$

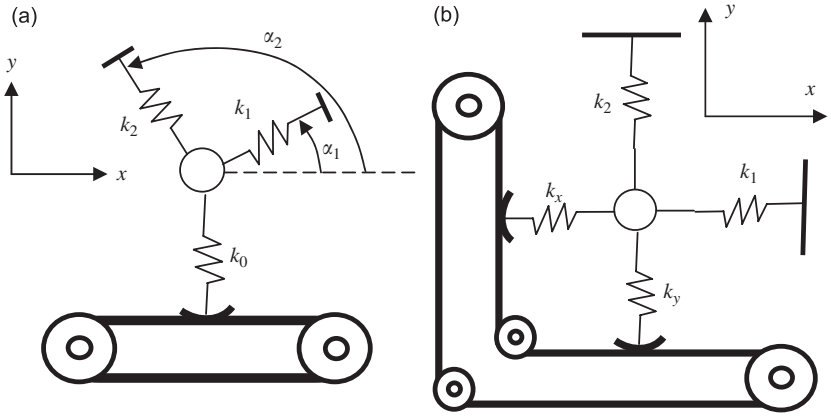


Fig. 3. Single-mass discrete models: (a) three spring model [11] with one contact spring and two system springs, (b) newly proposed four spring model with two orthogonal contact springs and two orthogonal system springs.

and, where $\eta$ is the friction factor with $k_1$, $k_2$, $k_x$ and $k_y$ being mass-normalized stiffness. In order to make two equations (19) and (32) equivalent, the system parameters of the discrete model are defined as the following:

$$k_1 = \omega_{2n-1}^2, \quad k_2 = \omega_{2n}^2, \tag{36}$$

$$k_x = \frac{k_c\theta_c\tilde{R}_n^z}{2}\left(1 + \frac{\sin(n\theta_c)}{n\theta_c}\right), \tag{37}$$

$$k_y = \frac{k_c\theta_c\tilde{R}_n^z}{2}\left(1 - \frac{\sin(n\theta_c)}{n\theta_c}\right), \tag{38}$$

$$\eta = \mu n\frac{\tilde{R}_n^\theta}{\tilde{R}_n^z}. \tag{39}$$

Here, the mathematically equivalent single-mass model with Eqs. (32)–(39) will be referred to as the disc doublet discrete model. It should be noted that the contact strain energies from orthogonal contact stiffness, $k_x$ and $k_y$ are equivalent to the modal contact strain energies from the disc cosine and sine modes, respectively. Also, the two system springs, $k_1$ and $k_2$ represent the component modal stiffness of the doublet mode pair. Even though the model-equivalency has been made in the absence of follower force terms, it retains accuracy in the actual disc brake system, as explained earlier. This disc doublet discrete model is relevant because it is the simplest two-degree-of-freedom model possibly representing a brake squeal model with physical geometry.

From the eigensolutions of Eq. (32), the equivalent critical friction factor can be written as

$$\eta_{\mathrm{cr}} = \frac{\left|(\omega_{2n-1}^2 - \omega_{2n}^2) + (k_x - k_y)\right|}{2\sqrt{k_x k_y}}. \tag{40}$$

The dynamic instability of this discrete system is exactly expressed by a component frequency separation and a contact stiffness separation in Eq. (40). It is clear that the smaller separation of component natural frequencies and the contact stiffness between two modes increases modal instability. Here, the contact stiffness separation, $\Delta k = |k_x - k_y|$ in the discrete system can be found from the contact span angle of the actual disc in Eqs. (37) and (38). Again, the contact stiffness separation in the disc doublet discrete model equivalently represents the difference between the modal contact strain energies of a doublet mode pair. Therefore, the minimal stiffness-coupled frequency separation addressed in the previous section can be understood in the way that if two modes in a doublet pair have the identical modal contact strain energy, the propensity of the modal instability due to the doublet mode reaches to the maximum level.

### 2.4. Finite element modal model

In this analysis, $N$ vibration modes are found from the finite element model of a physical brake rotor and two pads are assumed to be fixed as illustrated in Fig. 4. The transverse and circumferential displacements of the rotor are written in the following truncated modal expansion using the finite element model:

$$w(\vec{x},t) \cong \sum_{j=1}^{N}\phi_j^z(\vec{x})q_j(t), \quad v(\vec{x},t) \cong \sum_{j=1}^{N}\phi_j^\theta(\vec{x})q_j(t). \tag{41}$$

Following the analytical procedure, the contact forces are defined at every node on the contact surface of the rotor such that

$$\begin{Bmatrix} F_{\mathrm{top}} \\ N_{\mathrm{top}} \\ F_{\mathrm{bottom}} \\ N_{\mathrm{bottom}} \end{Bmatrix} = \begin{Bmatrix} \mu(p_o + k_c w_{\mathrm{top}}) \\ p_o + k_c w_{\mathrm{top}} \\ \mu(p_o - k_c w_{\mathrm{bottom}}) \\ p_o - k_c w_{\mathrm{bottom}} \end{Bmatrix}, \tag{42}$$

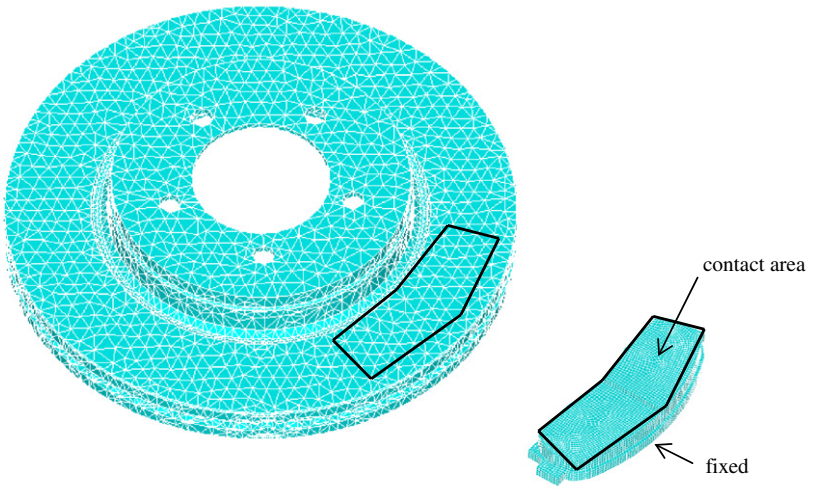


Fig. 4. Finite element disc and pad model.

where

$$\{q\} = \{q_1, q_2, \ldots, q_N\}^{\mathrm{T}}, \tag{43}$$

$$w_{\mathrm{top}}(\vec{x}_{\mathrm{top}}) \cong \sum_{j=1}^{N} \phi_j^z(\vec{x}_{\mathrm{top}}) q_j(t), \tag{44}$$

$$w_{\mathrm{bottom}}(\vec{x}_{\mathrm{bottom}}) \cong \sum_{j=1}^{N} \phi_j^z(\vec{x}_{\mathrm{bottom}}) q_j(t). \tag{45}$$

As previously noted, follower forces are not included in Eq. (42) as the contact forces are defined in the undeformed surface of the disc. By substituting Eqs. (42)–(45) into Eq. (13), the modal equations of motion for a $N$ degree-of-freedom model take the form of

$$\underline{\ddot{q}} + [\tilde{\omega}^2]\underline{q} + k_c[\tilde{A}]\underline{q} + \mu k_c[\tilde{B}_\theta]\underline{q} = 0, \tag{46}$$

where

$$\tilde{A}_{nm} = \int_{\mathrm{CS}} \{\phi_n^z(\vec{x}_{top})\phi_m^z(\vec{x}_{\mathrm{top}}) + \phi_n^z(\vec{x}_{\mathrm{bottom}})\phi_m^z(\vec{x}_{\mathrm{bottom}})\}\, \mathrm{d}A, \tag{47}$$

$$\tilde{B}_{nm}^{\theta} = \int_{CS} \{-\phi_n^{\theta}(\vec{x}_{\mathrm{top}})\phi_m^z(\vec{x}_{\mathrm{top}}) + \phi_n^{\theta}(\vec{x}_{\mathrm{bottom}})\phi_m^z(\vec{x}_{\mathrm{bottom}})\}\, \mathrm{d}A. \tag{48}$$

$\{\phi_n^z(\vec{x}_{\mathrm{top}})\}_{n=1,2,\ldots,N}$, $\{\phi_n^z(\vec{x}_{\mathrm{bottom}})\}_{n=1,2,\ldots,N}$, $\{\phi_n^{\theta}(\vec{x}_{\mathrm{top}})\}_{n=1,2,\ldots,N}$, $\{\phi_n^{\theta}(\vec{x}_{\mathrm{bottom}})\}_{n=1,2,\ldots,N}$ are the $n$th $(1 \times M)$ modal vectors in the transverse and circumferential directions, respectively, which contain modal information on every node of the top and bottom contact surface ($M$ is the number of elements by the discretization of contact surface) and $\{\omega_1, \omega_2, \ldots, \omega_N\}$ are the circular frequencies of the disc. The original modal vectors of all nodes in the finite element disc model are obtained by a modal analysis with ANSYS software. In this finite element model, the 56 vibration modes of the disc are retained. The contact surface between the disc and the brake pad lining is discretized into nearly 8000 elements and the area integration over contact surface is conducted by numerical calculation such as $\int_{\mathrm{CS}} \mathrm{d}A \cong \sum_{i=1}^{M} \Delta A_{\mathrm{cs}}$, as detailed in Ref. [10].

## 3. Numerical results

For a preliminary consideration, the results obtained from modal analysis and stability analysis of finite element model are presented first. Table 1 shows the natural frequencies of the finite element component disc

Table 1
Natural frequencies of the transverse doublet modes of the finite element disc brake with free-free boundary condition (Hz)

| $n$ | | | | | | |
|---|---|---|---|---|---|---|
| 2 | 3 | 4 | 5 | 6 | 7 | 8 |
| 976 | 2340 | 3863 | 5550 | 7362 | 9275 | 11 256 |
| 977 | 2341 | 3867 | 5552 | 7371 | 9282 | 11 276 |

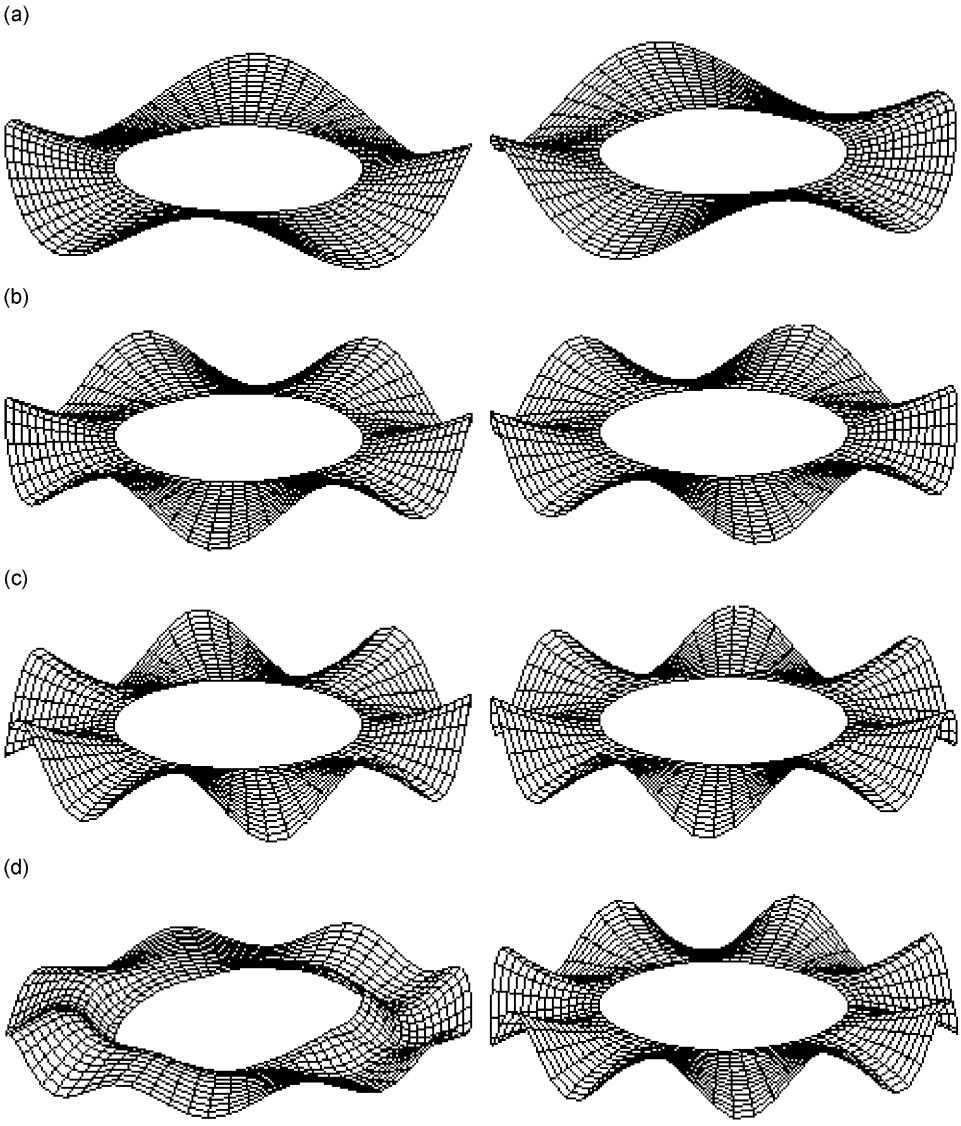


Fig. 5. Mode shapes on squeal frequencies for finite element disc brake at $\mu = 0.4$ and $k_c = k_{\text{nom}}$: (a) doublet mode pair ($n = 4$), (b) doublet mode pair ($n = 6$), (c) doublet mode pair ($n = 7$), and (d) nodal diameter mode ($n = 8$) and adjacent mode.

model, where some of doublet modes have the significant component frequency separation, for example, 9 Hz frequency separation for the 6th doublet mode. By solving for the eigensolutions of Eq. (46) and converting the mode shapes corresponding to unstable modes, the unstable modes can be identified. Shown in Fig. 5 are the mode shapes of unstable modes on squeal frequencies at $\mu = 0.4$ and $k_c = k_{\text{nom}}$. Of the four mode shapes presented in Fig. 5, the first three correspond to the transverse doublet modes leading to squeal. Therefore, the dynamic instability of these doublet modes deserves attention in the linear brake squeal analysis.

Here the contact geometry of the analytical model is simplified as an annular sector shape having a contact span angle, inner and outer radii as shown in Fig. 6 and system parameters are summarized in Table 2. The corresponding modal data is obtained by solving the boundary value problem as detailed in Eq. (4) and summarized in Table 3. For comparison between the results of our analytical model and the physical finite

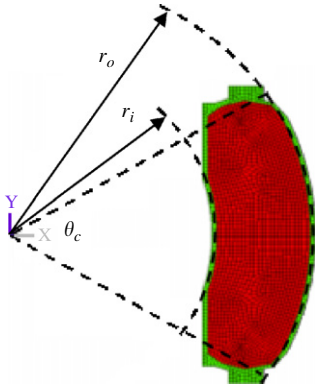


Fig. 6. Contact geometry of physical pad lining; contact span angle ($\theta_c$), inner radius ($r_i$), and outer radius ($r_o$).

Table 2
Nominal values of system parameters in the analytical disc model

| Parameter | Symbol | Value |
|---|---|---|
| Outer radius of the disc | $b$ | 150 mm |
| Inner radius of the disc | $a$ | 40 mm |
| Outer radius of contact area | $r_o$ | 142 mm |
| Inner radius of contact area | $r_i$ | 100 mm |
| Thickness of the disc | $h$ | 26 mm |
| Contact angle | $\theta_c$ | 62° |
| Young's modulus | $E$ | 88.9 GPa |
| Density | $\rho$ | 7150 kg/m$^3$ |
| Poisson's ratio | $v$ | 0.285 |
| Nominal contact stiffness | $k_{\text{nom}}$ | $0.35 \times 10^{11}$ N/m$^3$ |

Table 3
Frequencies and modal constants for the annular plate subject to clamped boundary condition at inner radius and free boundary condition at outer radius

| $n$ | 1 | 2 | 3 | 4 | 5 | 6 | 7 | 8 |
|---|---|---|---|---|---|---|---|---|
| $f_n$ | 1153 | 1447 | 2553 | 4318 | 6589 | 9308 | 12 461 | 16 040 |
| $A_n$ | 0.4440 | 1.0013 | 1.2512 | 1.4528 | 1.6428 | 1.8223 | 1.9925 | 2.1546 |
| $E_n$ | 0.6749 | 0.2232 | 0.0482 | 0.0097 | 0.0018 | 0.0003 | 0.0001 | 0.0000 |
| $B_n$ | 0.1326 | 0.1534 | 0.1041 | 0.0594 | 0.0332 | 0.0186 | 0.0105 | 0.0059 |
| $F_n$ | 0.5245 | 0.1619 | 0.0358 | 0.0075 | 0.0015 | 0.0003 | 0.0000 | 0.0000 |
| $\beta_n$ | 16.1987 | 18.1476 | 24.1023 | 31.3456 | 38.7159 | 46.0215 | 53.2484 | 60.4116 |

$A_n$, $E_n$, $B_n$, $F_n$ are normalized by modal masses.

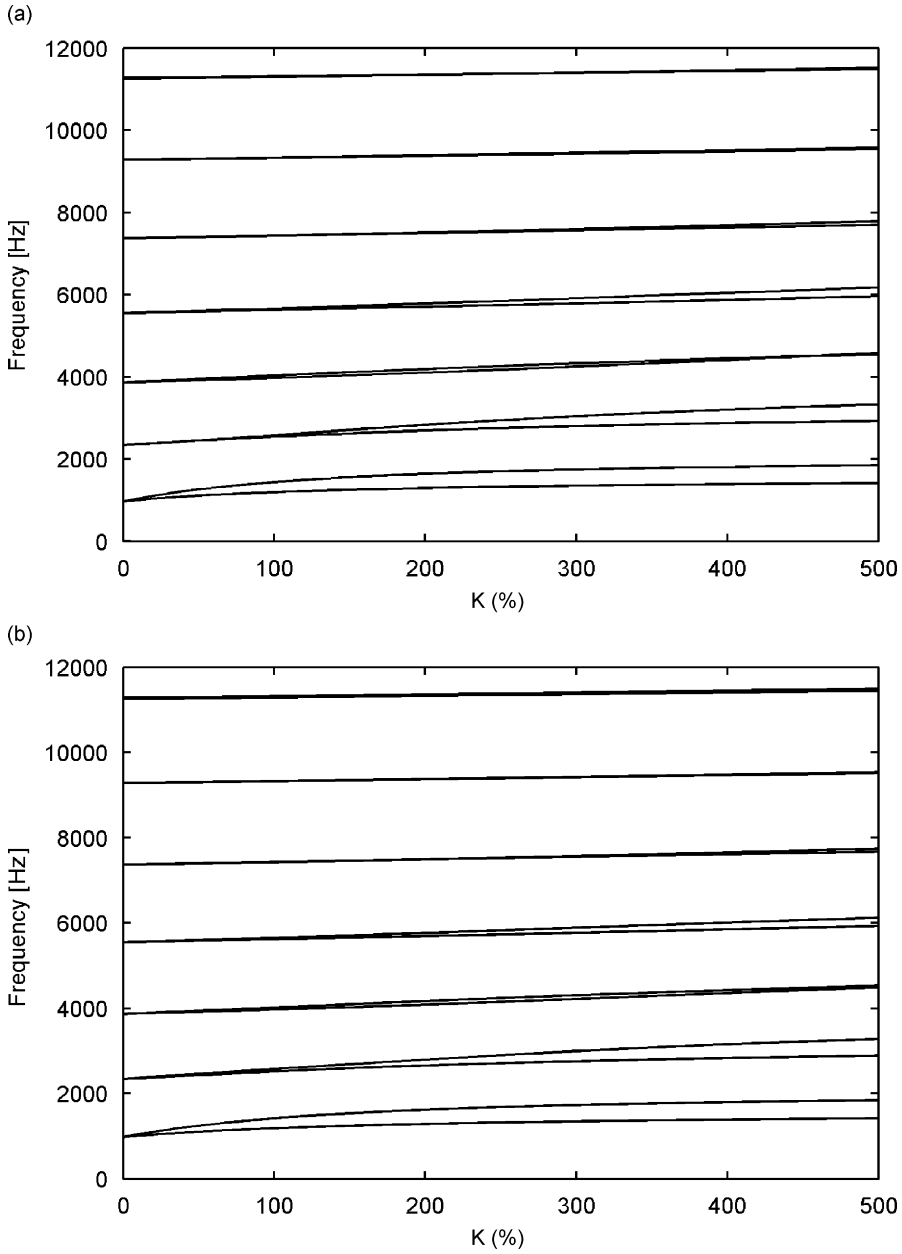


Fig. 7. Frequency loci with respect to contact stiffness variation on zero friction coefficient domain: (a) analytical multiple-mode model for the annular plate, and (b) finite element model of a car disc brake leaving off any modes except transverse doublet modes.

element disc model, the natural frequencies of the finite element disc model are brought into the analytical model. To demonstrate the validation of analytical solution, the eigensensitivity analysis associated with the variation of the contact stiffness is conducted. Fig. 7 illustrates that the stiffness-coupled frequency loci of the FE and analytical model are well approximated. The modal stability boundaries obtained from two models are also close as depicted in Fig. 8.

Another validation may be required for the analytical reduced-order model. The one-doublet mode model is based on the assumption that the modal influence from modes other than the doublet pair is weak enough to be neglected due to relatively large frequency separation, as opposed to the nearly zero frequency separation between two sine/cosine modes in the doublet pair. Fig. 9 illustrates that the eigensolution of the one-doublet

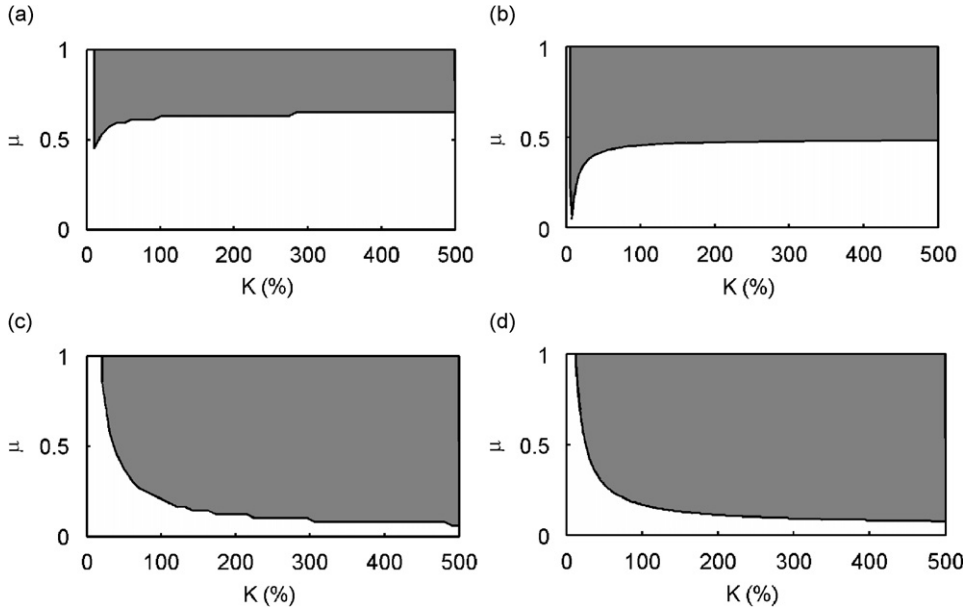


Fig. 8. Modal stability boundary of a single doublet mode pair solved by finite element model and analytical model; for $n = 4$, $\Delta f = 4(3863/3867\,\text{Hz})$: (a) finite element stability, (b) analytical stability; for $n = 6$, $\Delta f = 9(7362/7371\,\text{Hz})$, (c) finite element stability, and (d) analytical stability; dark region represents unstable region.

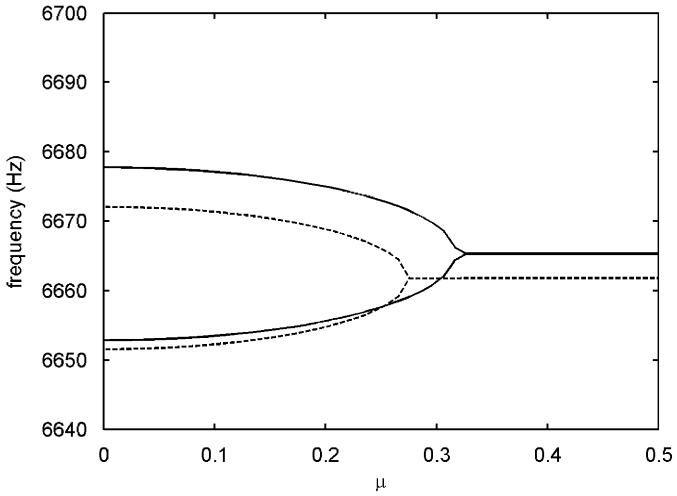


Fig. 9. Validation for the one-doublet mode model ($n = 5$) at $k_c = k_{\text{nom}}$; (—): multiple-mode model ($N = 16$), (––): one-doublet mode model.

mode model is well approximated to that of the multiple-mode model in terms of a mode-merging point as squeal onset.

The one-doublet mode model is now utilized to investigate mode-coupling squeal mechanism due to disc doublet modes. In order to account for the component frequency separations of the doublet modes in the physical finite element disc brake, the natural frequencies from the finite element modal analysis as shown in Table 1 are used. The critical issue is that the minimum level of a critical friction coefficient can be determined by the specific contact span angles as shown in Fig. 10. The results show that the contact span angle plays a key role on the squeal propensity of transverse doublet modes. Fig. 11 provides the stability diagram for the squeal propensity induced by a transverse doublet mode. The critical contact span angles for the doublet mode

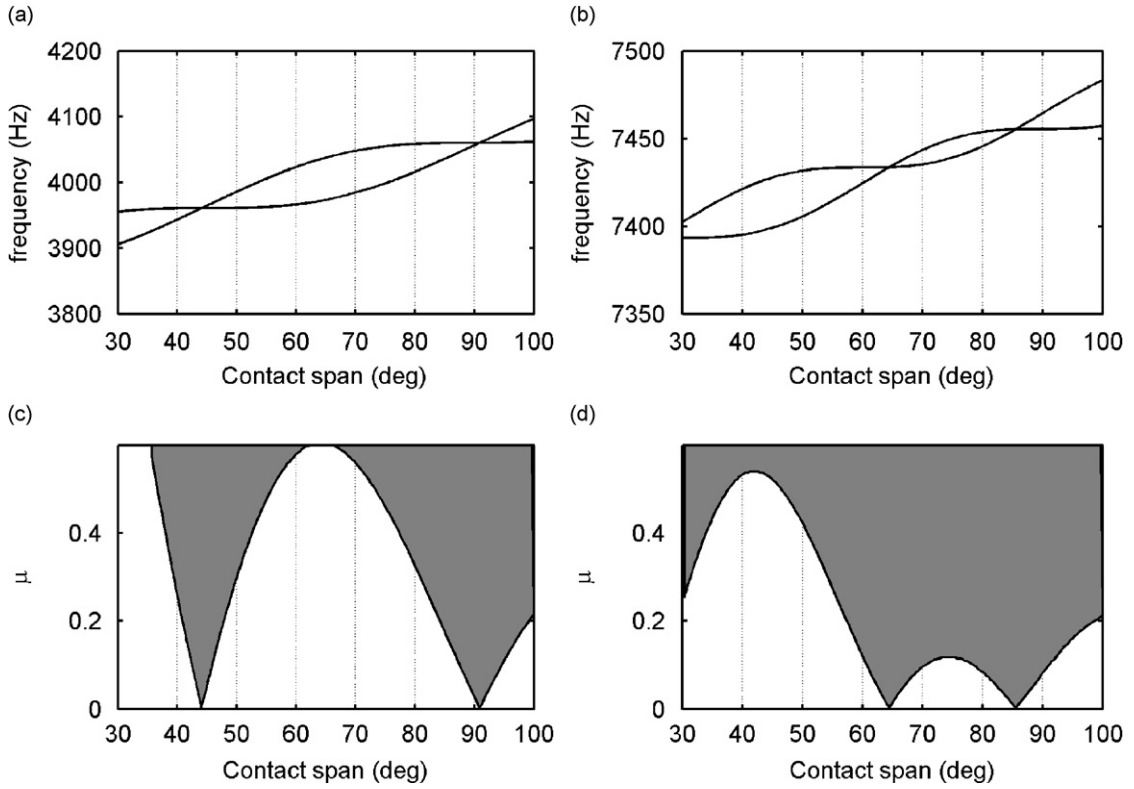


Fig. 10. Stability analysis with respect to the variation of contact span angle at $k_c = k_{\text{nom}}$; frequency loci of a doublet mode pair: (a) $n = 4$(3863/3867 Hz), (b) $n = 6$(7362/7371 Hz), stability region: (c) $n = 4$(3863/3867 Hz), and (d) $n = 6$(7362/7371 Hz); dark region represents unstable region.

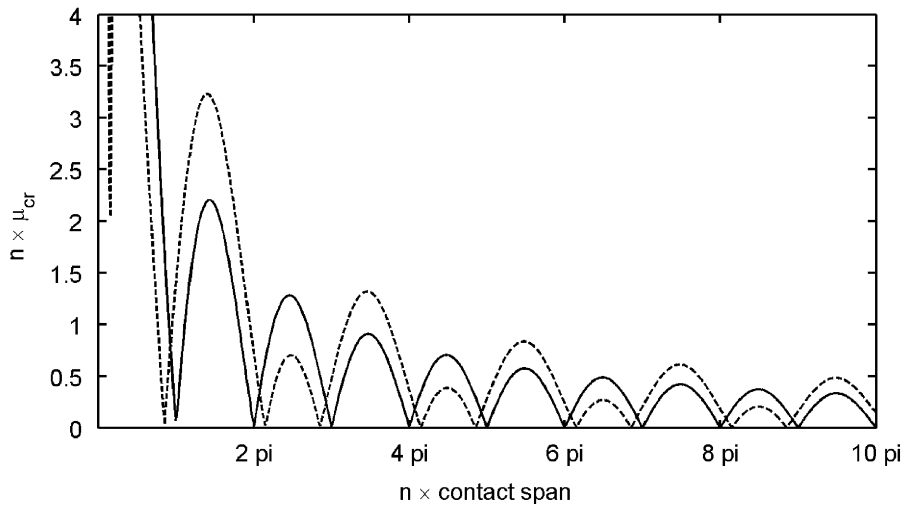


Fig. 11. Stability diagram for $n = 6$ with respect to $n\theta_c$ and $n\mu_{\text{cr}}$; (—): zero frequency separation (7371/7371 Hz), (––): non-zero frequency separation (7362/7371 Hz); the minimal values of $n\mu_{\text{cr}}$ correspond to $\sin(n\theta_c) = 0$ for a doublet mode with zero frequency separation.

pairs with zero component frequency separation ($\omega_{2n-1} = \omega_{2n}$) are shown to be periodic values as opposed to those of the doublet mode pairs with non-zero component frequency separation ($\omega_{2n-1} \neq \omega_{2n}$).

From the disc doublet discrete model, the role of the contact span angle is also demonstrated. Fig. 12 illustrates that the ratio of contact stiffness, $k_y/k_x$ in the disc doublet discrete model varies with respect to the

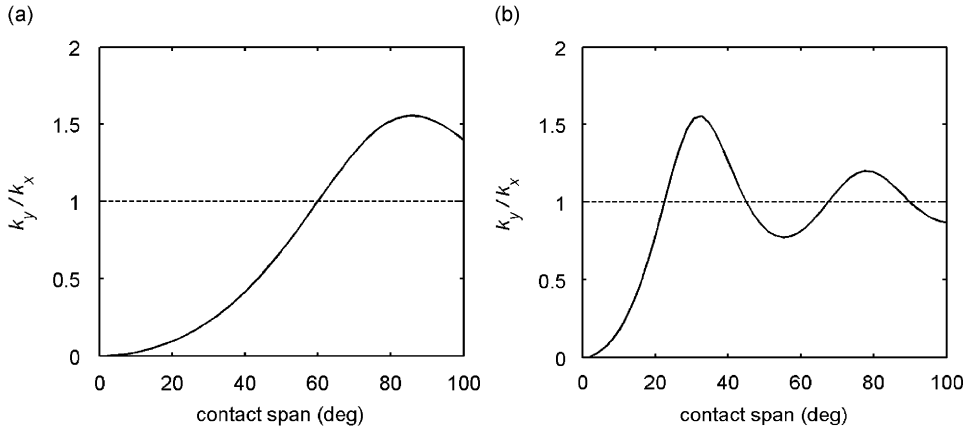


Fig. 12. The ratio of contact stiffness in the disc doublet discrete model with respect to the variation of contact span angle: (a) $n = 3$, (b) $n = 8$ contact stiffness separation becomes zero at $\sin(n\theta_c) = 0$.

variation of the physical contact span angle. As $k_y/k_x$ approaches to unity, the squeal propensity increases. Therefore, the critical contact span angles for the $n$th doublet mode model correspond to $k_y/k_x = 1$ in this figure.

In summary, corresponding to every transverse doublet mode is a critical contact span angles. Therefore, the contact span angle should be the substantial design parameter for controlling mode-coupling type squeal propensity in a car disc brake system. The squeal propensity can be decreased by designing the pad arc angle to avoid the critical contact span angles as described in Eq. (31). It should be noted that the component frequency separation of a doublet mode pair enforces to design the brake system more carefully since the critical contact span angles become dependent of contact stiffness.

## 4. Conclusions and discussion

The squeal mechanism of a thin disc with finite contact area has been studied analytically. The analytical model was validated by comparing its results with those of the finite element model of an actual disc brake system. The validation allowed us to investigate the squeal mechanism of an actual disc brake system through the use of the one-doublet mode model. The one-doublet mode model led to a closed-form solution which is used to explain how the stiffness-coupled (or component) frequency separation in a doublet mode pair influences on squeal propensity.

The closed-form solution and numerical calculation allowed the following conclusions to be drawn. First, for zero component frequency separation in a doublet mode, the highest squeal propensity arises at the specific contact span angles satisfying $\sin(n\theta_c) = 0$. If the component frequency separation in a doublet mode is not zero, the critical contact span angle will be the function of contact stiffness and the component frequency separation. The critical contact span angles can be obtained from simple numerical calculation of Eq. (31), and they are shown to be close values from the angles satisfying $\sin(n\theta_c) = 0$.

Furthermore, the one-doublet mode model of a disc has been equivalently expressed as a two-degree-of-freedom discrete model in the linear stability analysis. This simplified model is useful in explaining squeal mechanism due to the doublet mode pair of a disc rotor. From this model, it was seen that the modal contact strain energy is related to the propensity for modal instability, where the contact span angle is the influential parameter on the contact strain energy. This physical interpretation has been consistent with the relationship between mode-veering and modal instability previously mentioned in Refs. [9,10].

## Acknowledgments

This research is supported by Bosch Company, Ltd. The authors would like to thank Dr. Mohamed, Dr. Wang and Dr. Abdul-Hafiz for their support.

## References

[1] N.M. Kinkaid, O.M. O'Reilly, P. Papadopoulos, Automotive disc brake squeal, *Journal of Sound and Vibration* 267 (2003) 105–166.
[2] J.E. Mottershead, S.N. Chan, Flutter instability of circular discs with frictional follower loads, *Journal of Vibration and Acoustics* 117 (1995) 161–163.
[3] J.E. Mottershead, Vibration- and friction-induced instability in disks, *Shock and Vibration Digest* 30 (1998) 14–31.
[4] J. Flint, J. Hulten, Lining-deformation-induced modal coupling as squeal generator in a distributed parameter disc brake model, *Journal of Sound and Vibration* 254 (1) (2002) 1–21.
[5] J. Heilig, J. Wauer, Stability of a nonlinear brake system at high operating speeds, *Nonlinear Dynamics* 34 (2003) 235–247.
[6] H. Ouyang, J.E. Mottershead, Dynamic instability of an elastic disk under the action of a rotating friction couple, *Journal of Applied Mechanics* 71 (2004) 753–758.
[7] H. Ouyang, W. Nack, Y. Yuan, F. Chen, Numerical analysis of automotive disc brake squeal: a review, *International Journal of Vehicle Noise and Vibration* 1 (2005) 207–231.
[8] D.N. Vanderlugt, Analytical and Experimental Study of Automotive Disc Brake Squeal Vibration, Master Thesis, Purdue University, 2004.
[9] H.V. Chowdhary, A.K. Bajaj, C.M. Krousgrill, An analytical approach to model disc brake system for squeal prediction, CD-ROM, *Proceedings of DETC'01, DETC2001/VIB-21560*, ASME, Pittsburgh, PA, September 2001, pp. 1–10.
[10] J. Huang, C.M. Krousgrill, A.K. Bajaj, Modeling of automotive drum brake for squeal and parameter sensitivity analysis, *Journal of Sound and Vibration* 289 (2006) 245–263.
[11] N. Hoffmann, M. Fischer, R. Allgaier, L. Gaul, A minimal model for studying properties of mode-coupling type instability in friction induced oscillations, *Mechanics Research Communications* 29 (2002) 197–205.
[12] D. Hochlenert, G.S. Korspeter, P. Hagedorn, Friction induced vibrations in moving continua and their application to brake squeal, *Journal of Applied Mechanics* 74 (2007) 542–549.
[13] T.B. Gabrielson, Frequency constants for transverse vibration of annular disks, *Journal of the Acoustical Society of America* 105 (6) (1999) 3311–3317.